Journal of Alloys and Compounds 509 (2011) 2111–2115

Contents lists available at ScienceDirect

Journal of Alloys and Compounds

journal homepage: www.elsevier.com/locate/jallcom

Growth of AlN nanobelts, nanorings and branched nanostructures

H.B. Li[a], R. Wu[a,b], J. Li[a,b], Y.F. Sun[a,b], Y.F. Zheng[a,b], J.K. Jian[a,b,*]

[a] Department of Physics, Xinjiang University, Urumqi 830046, Xinjiang, PR China
[b] Key Lab for Solid State Physics & Devices, Xinjiang University, Urumqi 830046, Xinjiang, PR China

ARTICLE INFO

Article history:
Received 25 August 2010
Received in revised form 19 October 2010
Accepted 27 October 2010
Available online 4 November 2010

Keywords:
Nanostructured materials
Aluminum nitride
Vapor deposition

ABSTRACT

Single-crystalline AlN nanobelts, nanorings and branched nanostructures have been synthesized through a catalyst-free chemical vapor deposition (CVD) process employing Al power as starting material. The morphologies and microstructures of the as-prepared AlN nanostructures were characterized and it was found that the AlN nanobelts are well-crystallized with top/bottom surfaces of ±(0 0 1) planes of hexagonal AlN. The formation of AlN nanorings is accounted by the electrostatic polar charge model. The branched AlN nanostructures consist of nanobelt backbones and numerous nanorod branches which are all single crystals. The growth mechanism of the AlN nanostructures is discussed and a lateral secondary growth is suggested to address the formation of branched nanostructures. Photoluminescence (PL) spectrum of AlN nanobelts presents a defect-relative emission centered at 488 nm.

1. Introduction

Since the discovery of semiconducting oxides nanobelts [1], belt-like nanomaterials have attracted great attention due to their unique geometries, novel physical and chemical properties, and potential applications in nanoscale electronics and photonics [2–15]. Some devices including field-effect transistors [16], ultrasensitive gas sensors [17], and resonators [18] have been fabricated based on individual nanobelts. In the past decade, nanobelts of oxides (ZnO, CdO, SnO_2) [1,2], sulfides (ZnS, CdS) [3–5], III-nitrides (GaN, AlN) [6–10], and some other compounds (Ge_3N_4, SiC, Sb_2Te_3, CdSe) [11–14] have been synthesized by various of methods. Among them, AlN is an important semiconductor with some excellent properties such as high melting point and thermal conductivity, high piezoelectric response, excellent mechanical strength and chemical stability, and is the material suitable for a variety of applications in optoelectronic devices [19]. Also, AlN is a desired substrate for the fabrication of GaN/InN-based heterostructures because of its good lattice-match with GaN/InN. Some one-dimensional AlN nanostructures with unique optical and field-emission properties have been reported in the past several years. AlN nanocone and nanocolumn arrays have been synthesized by Hu et al. and our group [20,21]. Tang et al. synthesized AlN nanobelt arrays by an oxide-assisted vapor transport and condensation method at a relatively low temperature, and found that Fe_2O_3 is critical for growing the aligned AlN nanobelts [9]. By a cobalt-assisted thermal CVD process, Hu et al. reported the synthesis of AlN nanobelts through directly nitriding aluminum power at 1200 °C [10]. Duan and co-workers obtained AlN nanobelts and nanorings by evaporating aluminum alloy (aluminum 95 at%, manganese 5 at%) in ammonia/nitrogen atmosphere [22]. Recently, complex three-dimensional (3D) branched or hierarchical nanostructures assembled by nanowires or nanobelts have been of great interest due to their potential applications in nanodevices [23,24].

Despite some success in the growth of AlN nanostructures, it is still a significant challenge to achieve the fabrication of AlN nanostructures with controlled morphologies and surface architecture, in particular for AlN nanobelts and branched nanostructures, which have been rarely reported. Herein, we reported the controlled growth of AlN nanobelts, nanorings, and branched nanostructures by a catalyst-free CVD method employing the direction reaction between Al powder and ammonia under high temperature. No catalyst is intentionally involved in the synthesis. To the best of our knowledge, there is no report before on the growth of belt-like and branched nanobelts of AlN through such a facile CVD route. The results presented here indicate the feasibility of controlled growth of AlN nanostructures with desired morphologies, which should be helpful to facilitate their applications in nanodevices.

2. Experimental

The syntheses of AlN nanostructures were performed in a horizontal tube furnace under atmospheric pressure. In a typical run, 0.2 g of Al powder with a purity of 99.9% loaded in an alumina boat was placed in the center of the tube furnace. Several pieces of alumina substrates were placed right above the aluminum powder with a gap of 5 mm. No external catalyst was employed in the synthesis. First, an Ar flow of 200 standard cubic centimeter per minute (sccm) was introduced into the system after the alumina tube was pumped to a vacuum of 1×10^{-2} Pa. After the furnace was heated to 1400 °C at a heating rate of 10 °C/min, a NH_3 flow of 30 sccm

* Corresponding author at: Department of Physics, Xinjiang University, Urumqi 830046, Xinjiang, PR China. Tel.: +86 991 8583183; fax: +86 991 8582405.
E-mail address: jikangjian@gmail.com (J.K. Jian).

0925-8388/$ – see front matter © 2010 Elsevier B.V. All rights reserved.
doi:10.1016/j.jallcom.2010.10.159

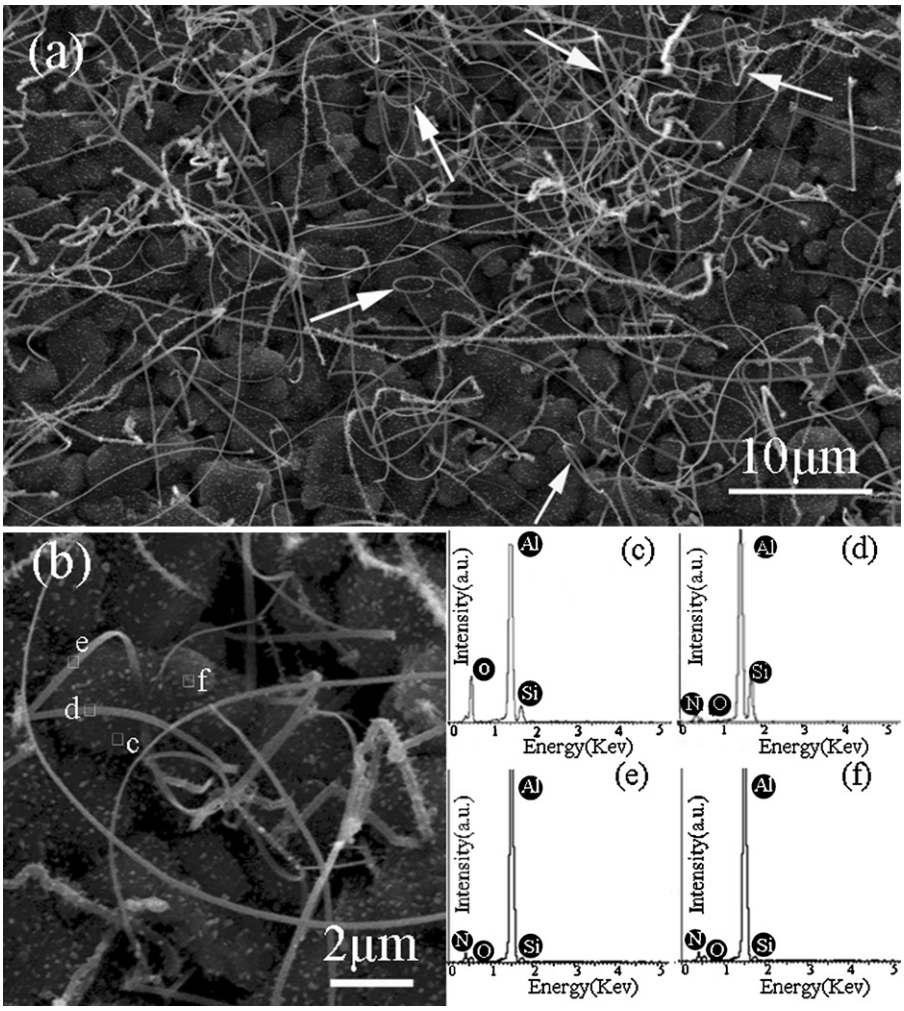

Fig. 1. (a) An overall SEM image of the as-synthesized AlN nanobelts and nanorings on Al_2O_3 substrate. Some AlN nanorings are indicated by arrowheads. (b) High magnification SEM image of AlN nanobelts. (c)–(f) EDX spectra obtained from boxed areas labeled as c, d, e, and f, respectively.

was started and maintained for 1 h. Then, the system was cooled to 800 °C naturally and the NH_3 flow was switched off. Finally, the system was cooled down to room temperature naturally under the Ar flow, and some white depositions were found on the substrates. A serial of control experiments were performed to reveal the growth progress of the nanostructures. The products were characterized by scanning electron microscopy (SEM, LEO 1430VP) equipped with an energy-dispersive X-ray (EDX) analyzer attachment, transmission electron microscopy (TEM, Hitachi H-600) and high-resolution transmission electron microscopy (HRTEM, JEOL JEM-2100). Photoluminescence (PL) spectrum of the product was taken at room temperature using the 325 nm of He–Cd laser with a Hitachi F-4500 spectrofluorometer.

3. Results and discussion

Fig. 1a is a low-magnification SEM image, giving an overall view of the morphology of the sample. One can see that the sample consists of a large quantity of wire-like structures with lengths of about tens of micrometers. It is worth noting that there are some ring-like structures in the sample, as indicated by the arrowheads. Fig. 1b is a high-magnification SEM image, indicating that these wire-like structures are nanobelts with the widths of 100–150 nm and thickness of about 10–30 nm. The lengths of the nanobelts can be tens of micrometers. Some nanobelts tend to bent itself along their longitudinal direction, showing good flexibility. In addition, it can be seen that some nanobelts have smooth surface and uniform width along their longitudinal direction while a part of the nanobelts have rough surface and branches. Apart from the nanobelts, a large number of nanoparticles are also found in the rough Al_2O_3 substrate, as labeled by the rectangle area f. To investigate the chemical compositions of the depositions, several EDX spectra are recorded from sites on the nanobelts, the nanoparticles and the bare area of substrate, which are labeled as c, d, e, f in Fig. 1b, respectively. The corresponding EDX spectra are shown in Fig. 1c–f, respectively. Fig. 1c is the EDX spectrum taken from the bare region of substrate (region c). Al and O signals can be detected and quantitative analysis indicates their atomic ration is close to 2:3. The result is consistent with the substrate of Al_2O_3. The weak peak of Si element may come from the purity of Al_2O_3 substrate. After deducting the O component which probably comes from residual oxygen or water in the system, the EDX spectra (Fig. 1d–f) taking from the nanobelts and nanoparticles are mainly composed of Al and N elements with the molar ratio of about 0.99:1. The EDX analysis indicates that both the nanobelts and nanoparticles are near stoichiometric AlN.

TEM, HRTEM and select area electron diffraction (SAED) were conducted to further investigate the microstructure of the AlN nanobelts. A TEM bright-field image is presented in Fig. 2a, displaying its smooth surface and uniform width of about 100 nm. Fig. 2b shows an atomic resolved HRTEM of the edge part of the nanobelt, revealing its high-crystalline structure free of defect. Crystal planes with spacing of about 0.27 nm and 0.16 nm can be measured in the HRTEM image, which can be assigned to {1 1 0} and {1 0 0} planes of hexagonal AlN (ICDD PDF No: 25-1133). This shows that the nanobelts grow along [2 1 0]. The SAED pattern shown in Fig. 2d of the nanobelt can be indexed to the [0 0 1] zone of hexagonal AlN.

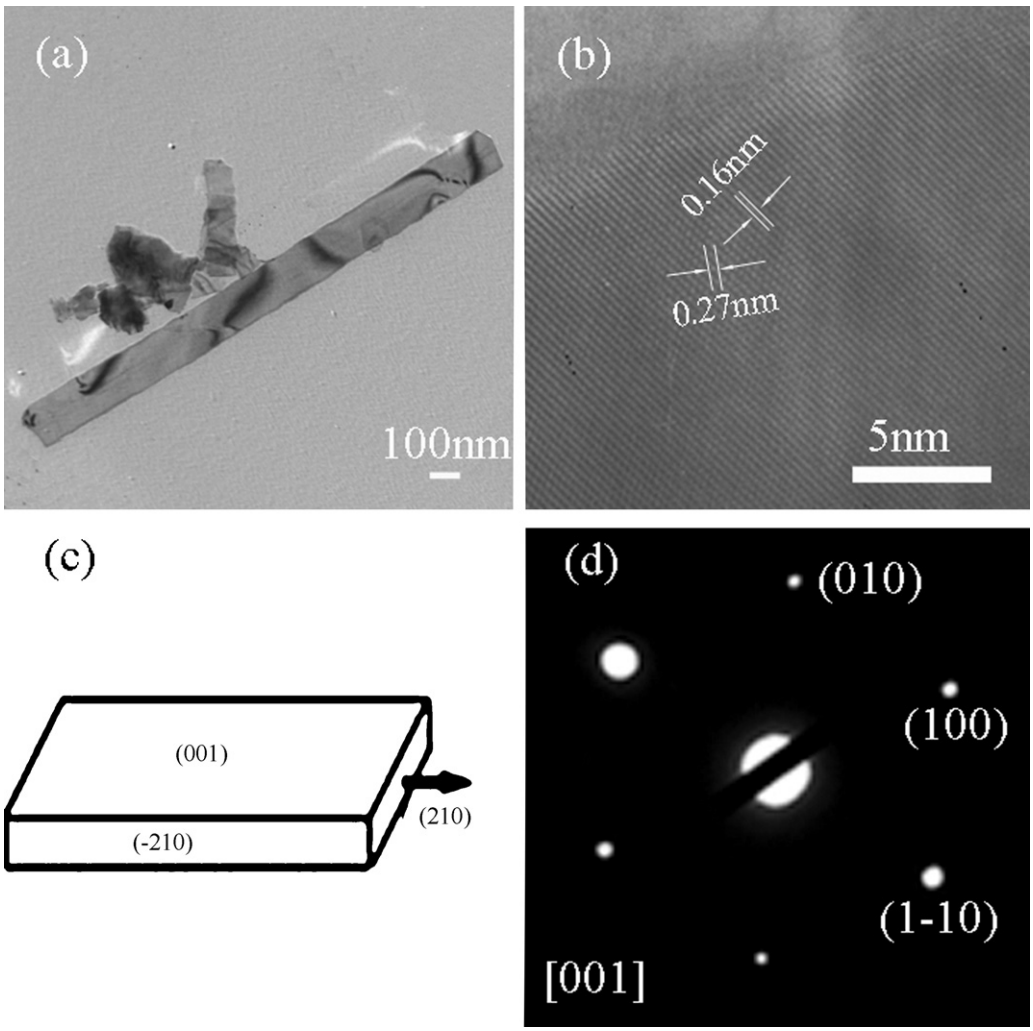

Fig. 2. (a) TEM image of one AlN nanobelt, (b) HRTEM image of the AlN nanobelt, indicating that the nanobelt is single with a growth direction of [2 1 0]. (c) The structural model of the AlN nanobelt. (d) The select area electron diffraction (SAED) pattern.

The SAED pattern further indicates that the AlN nanobelt grows along [2 1 0] and its top/bottom surface is ±(0 0 1) planes of h-AlN, so-called polarized-surface-terminated nanobelts [25]. Based on the results of HRTEM and SAED, the crystallographic illustration of the nanobelt is displayed in Fig. 2c, which is same with the case of ZnO nanobelts [25]. The morphology and structure of the AlN nanobelts imply the feasibility of the formation of ring-like structure by self-bending of the nanobelts which will be discussed below.

As indicated in Fig. 1a, there are some nanorings in the sample. Fig. 3a and b are high-magnification SEM images depicting the detailed morphological feature of the nanorings. It can be seen that the two nanorings are formed by the bending of nanobelts with uniform width and thickness. It is worth noting that Ref. [22] has reported AlN nanorings formed by bending of nanowires. The diameters of the nanorings are about 2.8 μm and 4.4 μm, respectively. According to the above TEM analysis and previous report of ZnO nanorings [25], the formation of AlN nanoring can be interpreted on the basis of electrostatic polar charge model that has been employed to illustrate the formation of ZnO, AlN and GaN nanorings [22,25,26]. In brief, the top/bottom surfaces of the ±(0 0 1) dominated AlN nanobelts would be charged with positive and negative charges by spontaneous polarization due to its noncentral symmetry structure. To minimize the electrostatic interaction energy among the polar charges, the nanobelts dominated by ±(0 0 1) planes tend to fold over. At the same time, the elastic deformation resulting from rolling a ring will increase the elastic energy. When the increase of the electrostatic energy dominates, the nanobelts will trend to roll up to form ring-like structure upon their growing along [2 1 0].

It is interesting to find that there are a large amount of branched-nanobelts at another region of the substrate. Fig. 4a shows a SEM image of the AlN branched-nanobelts, revealing that those nanostructures are tens of microns in length. A high-magnification SEM image (Fig. 4b) displays the morphological features of one typical branched nanobelt. One can see that there are many short nanorods grown on the center backbone which is a nanobelt with a width about 150–200 nm. The length and diameter of these small lateral branch nanorods are about 150–250 nm and 15–150 nm, respectively. As seen from the TEM image of a branched-nanobelt in Fig. 4c, those branches randomly distribute on the backbone nanobelt. The HRTEM image of one nanorod-branch is shown in Fig. 4d, indicating the branch is single crystal. Such branched nanobelts are different with previous reported nanoarchitectures that were self-assembled by AlN nanorods [23].

To examine the morphological evolution of AlN branched nanostructures, some control experiments were carried out with different growth duration while keeping other parameter fixed. Seen from Fig. 5a, a few of AlN nanoparticles have formed on the

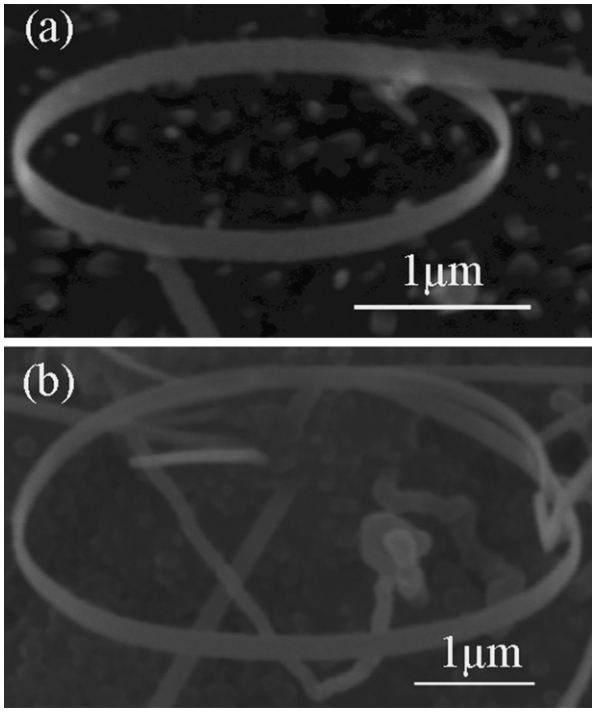

Fig. 3. (a) and (b) SEM image of individual nanorings.

surface of nanobelts with growth duration of 10 min. When the growth time was prolonged to 30 min, the branch-like structures become clear with higher density, as shown in Fig. 5b. When the growth time increased to 1 h (Fig. 5c), the nanorod branches completely grew on the side-surface of the nanobelts forming branched one-dimensional (1D) nanostructure.

Nowadays, the vapor-phase growth of 1D nanomaterials have been mainly accounted by catalyst-assisted vapor–liquid–solid (VLS) or vapor–solid (VS) process [27]. In our case, the formation of the nanobelts and branched nanostructures should be addressed by a vapor–solid mechanism [1,20,23] because that no external catalyst was involved in the present synthesis and no liquid-phase intermediate was observed. It has been pointed out that the anisotropic crystal structure of hexagonal AlN should be responsible for the formation of 1D AlN nanostructures through a VS process [20,23]. The related process can be briefly depicted as follows. Firstly, Al vapor generated at high temperature reacted with NH_3, which formed AlN species. Secondly, these AlN species were transported to substrates and precipitated from vapor phase when the vapor system became supersaturation. Finally, AlN crystals nucleated and grew into 1D nanostructures under proper growth conditions due to its anisotropic crystal structure. Deducing from the time-dependent synthesis, it is believed that the lateral secondary growth results in the formation of the AlN branched nanostructures synthesized here. With the growth of AlN nanobelts, the subsequent AlN species probably adsorbed on the side surfaces of those AlN nanobelts and epitaxialy grew into small

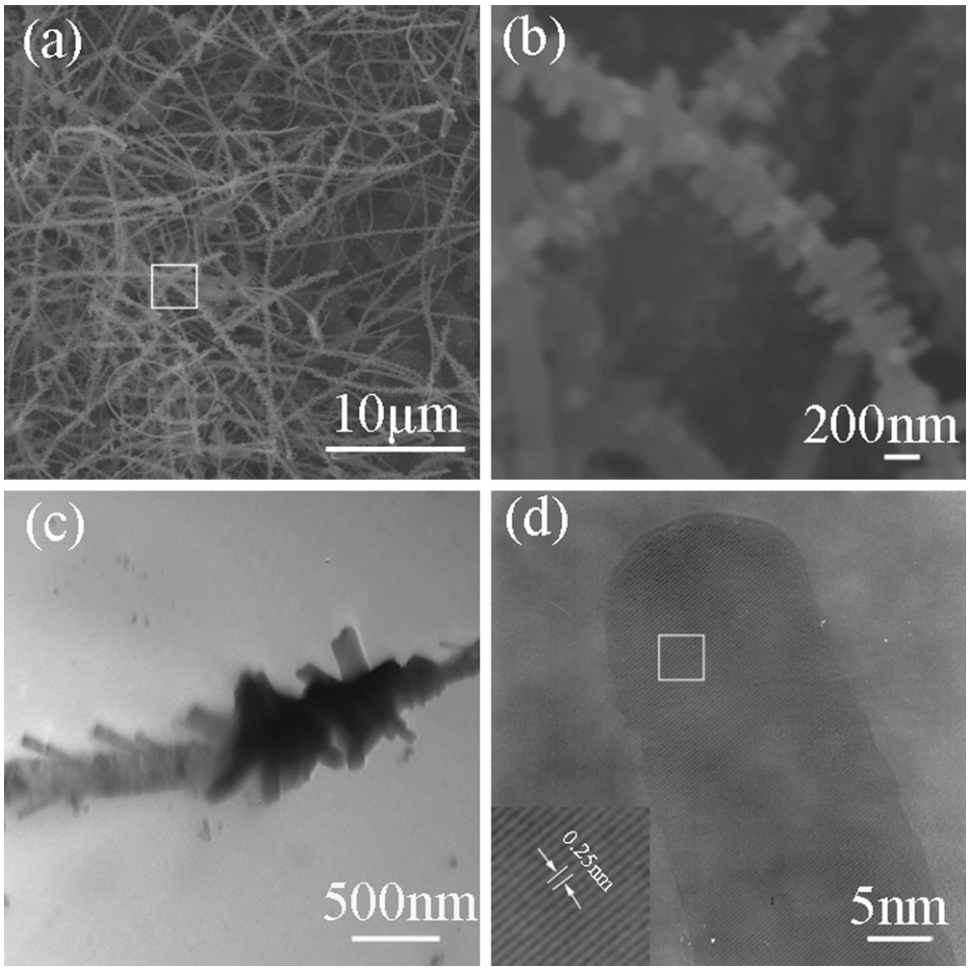

Fig. 4. (a) SEM image of the branched AlN nanostructures. (b) High magnification SEM image of the boxed area in (a). (c) TEM image of a single AlN branched nanostructure showing its branches grown randomly on the side of backbone. (d) HRTEM image of a nanorod branch. Inset: enlarged image of the box area, indicating single-crystalline structure of the nanorods.

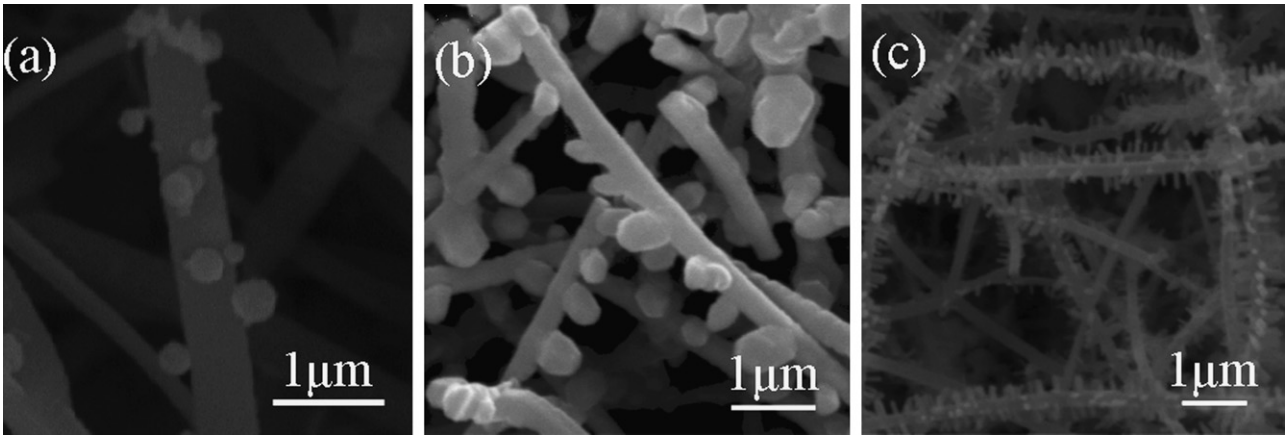

Fig. 5. SEM images of AlN branched nanostructures grown with different durations (a) 10 min (b) 0.5 h (c) 1 h.

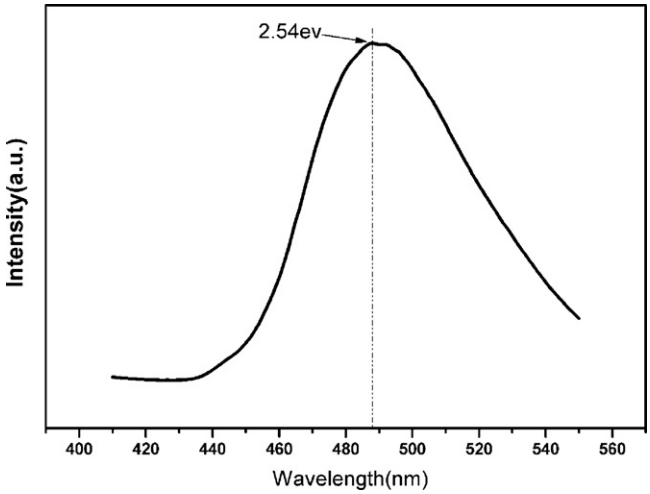

Fig. 6. PL spectrum of AlN nanobelts.

nanobranches, i.e. lateral secondary growth, leading in the formation of these branched nanostructures.

Fig. 6 presents the PL spectrum of the AlN nanobelts, which has a broad emission band centered at 488 nm (2.54 ev) similar to the PL spectra of AlN nanocones and nanoflowers [20,21,28]. The direct band gap emission of the AlN nanobelts is not seen here duo to the detection limitation. Obviously, the band should not be due to the bad gap emission of AlN, but is referred to as defect-related emission. Literatures [29] suggested that nitrogen vacancy or impurity level should be responsible for the emission.

4. Conclusions

In summary, a facile CVD technique was employed to synthesize AlN nanobelts, nanorings and branched nanostructures without the assistance of catalyst. SEM observations indicate that the AlN nanobelts have uniform morphology with length of about tens of microns. The AlN branched nanostructures are composed of nanobelt backbones and a large number of nanorod branches, which is a new morphology of AlN nanostructures. TEM analyses reveal single crystal nature of the AlN nanostructures and their growth is discussed. A broad blue emission is observed in the PL spectrum of AlN nanobelts, suggesting their potential applications in light emitting devices [20].

Acknowledgment

This work is supported by the National Natural Science Foundation of China (grant Nos. 50862008, 10864004).

References

[1] Z.W. Pan, Z.R. Dai, Z.L. Wang, Science 291 (2001) 1947–1949.
[2] R.S. Yang, Z.L. Wang, J. Am. Chem. Soc. 128 (2006) 1466–1467.
[3] P. Hu, Y. Liu, L. Fu, L. Cao, D. Zhu, J. Phys. Chem. B 108 (2004) 936–938.
[4] T. Gao, H.Q. Li, T.H. Wang, Appl. Phys. Lett. 86 (2005) 17315–173107.
[5] J.S. Jie, W.J. Zhang, Y. Jiang, X.M. Meng, Y.Q. Li, S.T. Lee, Nano Lett. 6 (2006) 1887–1892.
[6] J.Y. Li, Z.Y. Qiao, X.L. Chen, Y.G. Cao, Y.C. Lan, C.Y. Wang, Appl. Phys. A 71 (2000) 587–588.
[7] J.Y. Li, Z.Y. Qiao, X.L. Chen, Y.G. Cao, M.J. He, J. Phys.: Condens. Matter 13 (2001) L285–L289.
[8] S.Y. Bae, H.W. Seo, J. Park, H. Yang, S.A. Song, Chem. Phys. Lett. 365 (2002) 525–529.
[9] Y.B. Tang, H.T. Cong, F. Li, H.M. Cheng, Diam. Relat. Mater. 16 (2007) 537–541.
[10] Q. Wu, Z. Hu, X.Z. Wang, Y.N. Lu, Y. Chen, J. Phys. Chem. B 107 (2003) 9726–9729.
[11] C. Ma, D. Moore, Z.L. Wang, Adv. Mater. 15 (2003) 228–231.
[12] C. Ma, Y. Ding, D. Moore, X. Wang, Z.L. Wang, J. Am. Chem. Soc. 126 (2004) 708–709.
[13] W.D. Shi, J.B. Yu, H.S. Wang, H.J. Zhang, J. Am. Chem. Soc. 128 (2006) 16490–16491.
[14] J.S. Tsai, F.R. Chen, J.J. Kai, C.C. Chen, R.T. Huang, M.S. Wang, G.C. Huang, G.G. Guo, M.U. Yu, J. Appl. Phys. 95 (2004) 2015–2019.
[15] M.S. Hu, W.M. Wang, T.T. Chen, L.S. Hong, C.W. Chen, C.C. Chen, Y.F. Chen, K.H. Chen, L.C. Chen, Adv. Funct. Mater. 16 (2006) 537–541.
[16] L.J. Zhang, J.M. Du, B.X. Han, Z.M. Liu, T. Jiang, Z.F. Zhang, Angew. Chem. Int. Ed. 45 (2006) 1116–1119.
[17] J.C. Johnson, H.J. Choi, K.R. Knutsen, R.D. Schaller, P. Yang, R.J. Saykally, Nat. Mater. 1 (2002) 106–110.
[18] H. Yan, J. Johnson, M. Law, R. He, K. Knutsen, J.R. Mckinney, J. Pham, R. Saykally, P.D. Yang, Adv. Mater. 15 (2003) 1907–1911.
[19] S. Strite, H. Morkoc, J. Vac. Sci. Technol. B 10 (1992) 1237–1266.
[20] C. Liu, Z. Hu, Q. Wu, X.Z. Wang, Y. Chen, H. Sang, J.M. Zhu, S.Z. Deng, N.S. Xu, J. Am. Chem. Soc. 127 (2005) 1318–1322.
[21] H.B. Li, W.J. Wang, B. Song, R. Wu, J. Li, Y.F. Sun, Y.F. Zheng, J.K. Jian, J. Alloys Compd. 503 (2010) L34–L39.
[22] J.H. Duan, S.G. Yang, H.W. Liu, J.F. Gong, H.B. Huang, X.N. Zhao, J.L. Tang, R. Zhang, Y.W. Du, J. Cryst. Growth 283 (2005) 291–296.
[23] L.W. Yin, Y. Bando, Y.C. Zhu, M.S. Li, Y.B. Li, D. Golberg, Adv. Mater. 17 (2005) 110–114.
[24] W.W. Lei, D. Liu, J. Zhang, P.W. Zhu, Q.L. Cui, G.T. Zou, Cryst. Growth. Des. 3 (2009) 1489–1493.
[25] X.Y. Kong, Z.L. Wang, Nano Lett. 3 (2003) 1625–1631.
[26] J.K. Jian, Z.H. Zhang, Y.P. Sun, M. Lei, X.L. Chen, T.M. Wang, C. Wang, J. Cryst. Growth 303 (2007) 427–432.
[27] Y.N. Xia, P.D. Yang, Y.G. Sun, Y.Y. Wu, B. Mayers, B. Gates, Y.D. Yin, F. Kim, H.Q. Yan, Adv. Mater. 15 (2003) 353–389.
[28] F. Zhang, Q. Wu, X.B. Wang, N. Liu, J. Yang, Y.M. Hu, L.S. Yu, X.Z. Wang, Z. Hu, J.M. Zhu, J. Phys. Chem. C 113 (2009) 4053–4058.
[29] Y.G. Cao, X.L. Chen, Y.C. Lan, J.Y. Li, T. Xu, Y.P. Xu, Q.L. Liu, J.K. Liang, J. Cryst. Growth 213 (2002) 198–202.